

Disrupted Topological Organization in White Matter Structural Networks in Amnestic Mild Cognitive Impairment: Relationship to Subtype¹

Ni Shu, PhD
Ying Liang, MS
He Li, PhD
Junying Zhang, MS
Xin Li, MS
Liang Wang, PhD
Yong He, PhD
Yongyan Wang, BS
Zhanjun Zhang, MD

¹From the State Key Laboratory of Cognitive Neuroscience and Learning, Beijing Normal University, 19 Xijiekouwai St, Beijing 100875, P. R. China (N.S., Y.L., J.Z., X.L., Y.H., Z.Z.); Institute of Basic Research in Clinical Medicine, China Academy of Traditional Chinese Medicine, Beijing, P. R. China (H.L., Y.W.); and Princeton Neuroscience Institute, Princeton University, Princeton, NJ (L.W.). Received November 7, 2011; revision requested February 9, 2012; revision received April 20; accepted May 4; final version accepted May 8. Supported by the National Science Foundation of China (grant nos. 30873458, 81173460, and 81000633), Project of Institute of Basic Research in Clinical Medicine, China Academy of Chinese Medical Sciences (grant no. 20175), the Fundamental Research Funds for the Central Universities (grant no. 248-105102), Program for New Century Excellent Talents in University (grant no. NCET-10), Program for Excellent Doctoral Dissertation Foundation (grant no. 2007B7) and Project of Institute of Basic Research in Clinical Medicine (grant no. 20175). **Address correspondence to Z.Z.** (e-mail: zhang_rzs@bnu.edu.cn).

© RSNA, 2012

Purpose:

To investigate the topological alterations of whole-brain white matter structural connectivity in patients with different types of amnestic mild cognitive impairment (aMCI), including single-domain (SD) and multidomain (MD) aMCI, and to explore the relationship of such connectivity with neuropsychologic performance.

Materials and Methods:

This study was approved by the institutional review board of Imaging Center for Brain Research, Beijing Normal University. Written informed consent was obtained from each participant. The present study involved 38 patients with aMCI (SD aMCI, $n = 18$; MD aMCI, $n = 20$) and 36 age- and sex-matched healthy control subjects. White-matter connective architecture in each participant was depicted with diffusion-weighted MR imaging and represented in terms of a connectivity matrix by using a deterministic tractography method. Graph theory-based analyses were then performed to characterize brain network properties.

Results:

The global topological organization of white matter networks was significantly disrupted in patients with MD aMCI ($P < .01$ for all) but not in those with SD aMCI, as compared with control subjects. Connectivity impairment in patients with MD aMCI was found in the temporal, frontal, and parietal cortices ($P < .05$, corrected). MD aMCI had decreased network efficiency relative to SD aMCI ($P = .016$), with the most pronounced differences located in the frontal cortex ($P < .01$ for all). Strong associations between cognitive impairments and disrupted topological features (global, $P < .05$; regional, $P < .002$) were identified in patients with aMCI.

Conclusion:

The present study suggests early onset disruption of whole-brain white matter connectivity in patients with aMCI, especially in those with the MD subtype, supporting the view that MD aMCI is a more advanced form of disease than is SD aMCI. Moreover, cognitive correlations with topological network properties suggest their potential use as markers to assess the risk of Alzheimer disease.

© RSNA, 2012

Supplemental material: <http://radiology.rsna.org/lookup/suppl/doi:10.1148/radiol.12112361/-/DC1>

Mild cognitive impairment (MCI) is a diagnosis made in individuals who have cognitive impairments beyond what is expected for their age and education but that do not substantially interfere with their daily activities (1). In particular, amnesic MCI (aMCI) is considered a transition phase between normal aging and the onset of Alzheimer disease (AD) (2). According to the number of affected cognitive domains, patients with MCI can be further categorized as having single-domain (SD) or multidomain (MD) disease (3). In the context of aMCI, the SD aMCI subtype indicates a relatively selective episodic memory impairment; this is in contrast to the MD aMCI subtype, which indicates substantial deficits in at least one other cognitive domain (3).

In the past decade, magnetic resonance (MR) imaging techniques have been used to assess brain structural and functional alterations in patients with aMCI (4–6). For various aMCI subtypes, morphologic changes have

been reported (7–11). More widespread impaired gray matter regions were involved in the MD group than in the SD group, suggesting MD aMCI may be more advanced than SD aMCI, a fact that is also supported by the finding of a higher risk of conversion to AD in patients with MD aMCI than in those with SD aMCI (12).

Despite these advances, little is known about the alterations in the white matter (WM) as a secondary degenerative process in these patients from a system level. Recent studies have suggested that whole-brain WM connectivity can be reconstructed with diffusion MR imaging tractography and modeled by network approaches (13–15). Graph theoretical analysis revealed that WM networks exhibit many important topological properties, such as small worldness (16,17). Relatively recently, several studies have examined AD-related alterations of the topological organization in whole-brain networks, implying disrupted integration of the system (18–21). To our knowledge, only one study examined the topological properties of the structural brain network in patients with MCI; in that study, researchers calculated cross correlations in gray matter thickness derived from structural MR imaging (19). However, no studies reported aMCI-related changes in WM brain networks or investigated the topological differences among aMCI subtypes.

In this study, we used diffusion-tensor imaging and deterministic tractography to construct the WM structural networks in patients with aMCI and healthy control subjects. The purpose of this study was to investigate the topological alterations of whole-brain WM structural connectivity in patients with different types of aMCI and to explore the relationship of such connectivity with neuropsychological performance.

Materials and Methods

This study was approved by the institutional review board of the Imaging

Center for Brain Research, Beijing Normal University. Written informed consent was obtained from each participant.

Participants

We are conducting a 5-year longitudinal project that was started in October 2009, the goal of which is to identify neuroimaging biomarkers for MCI and AD. MR imaging data acquired from October 2009 to September 2010 were analyzed in the present study. Clinical and neuropsychological assessments were performed by expert neurologists blinded to the results of MR imaging (H.L., Z.Z.; 5 and 13 years of experience, respectively, in clinical neurology). Participants were included if they met the following criteria: (a) age of 50–85 years, (b) at least 6 years of education, and (c) a score of 24 or higher on the Chinese version of the Mini-Mental Status Examination (MMSE) (22). The exclusion criteria were as follow: (a) structural abnormalities other than cerebrovascular lesions—such as

Advances in Knowledge

- Application of graph theory principles to neuroimaging data offers a powerful approach with which to characterize and quantify large-scale structural and functional networks of the brain.
- Topological organization of white matter structural networks was significantly disrupted ($P < .05$) in patients with amnesic mild cognitive impairment (aMCI), especially in those with the multidomain subtype, representing aberrant interconnections between pairs of gray matter regions.
- The disrupted network properties were correlated with the clinical severity and neuropsychological performance of aMCI patients ($P < .05$), suggesting that network measures may be used as markers to assess the risk of conversion of MCI to Alzheimer disease.

Published online before print

10.1148/radiol.12112361 Content code: **NR**

Radiology 2012; 265:518–527

Abbreviations:

ACG = anterior cingulate gyrus
 AD = Alzheimer disease
 aMCI = amnesic MCI
 ANOVA = analysis of variance
 ITG = inferior temporal gyrus
 MCI = mild cognitive impairment
 MD = multidomain
 MFG = middle frontal gyrus
 MMSE = Mini-Mental State Examination
 SD = single domain
 SFG_{dor} = dorsal superior frontal gyrus
 SFG_{med} = medial superior frontal gyrus
 WM = white matter

Author contributions:

Guarantors of integrity of entire study, N.S., H.L., Y.H., Y.W., Z.Z.; study concepts/study design or data acquisition or data analysis/interpretation, all authors; manuscript drafting or manuscript revision for important intellectual content, all authors; approval of final version of submitted manuscript, all authors; literature research, N.S., Y.L., J.Z., X.L., Y.H., Y.W., Z.Z.; clinical studies, N.S., Y.L., J.Z., Y.H., Z.Z.; statistical analysis, N.S., L.W., Y.H., Z.Z.; and manuscript editing, N.S., H.L., Y.H., Y.W., Z.Z.

Conflicts of interest are listed at the end of this article.

tumors, subdural hematomas, and contusions due to previous head trauma—that could impair cognitive function; (b) history of addictions, neurologic or psychiatric diseases, or treatments that would affect cognitive function; (c) large vessel disease, such as cortical or subcortical infarcts and watershed infarcts; and (d) diseases with WM lesions, such as normal pressure hydrocephalus and multiple sclerosis. In all subjects with aMCI, the diagnosis was made according to the criteria of Petersen (23), which included subjective memory complaints, cognitive impairments in memory (1.5 standard deviations below the age- and education-adjusted norm on the Auditory Verbal Learning Test [or AVLT] [24]), normal general cognitive function (MMSE score no lower than 24, except in two patients who scored 22 and 23), and preserved activities of daily living (score of 0 on the Activities of Daily Living [or ADL] scale [25]). If episodic memory was the only area of impairment, patients were considered to have SD aMCI. If any additional cognitive domains were affected (1.5

standard deviations below age norms), patients were considered to have MD aMCI.

A total of 86 participants fulfilled the inclusion criteria, including 46 patients with aMCI and 40 age- and sex-matched healthy control subjects. Of the 46 patients with aMCI, five were excluded due to cerebral tumor, cerebral infarct, and leukoencephalopathy, and three were excluded because of poor image quality. Of the 40 healthy control subjects, two dropped out during MR imaging, and two were excluded because of poor image quality. Finally, 18 patients with SD aMCI, 20 patients with MD aMCI, and 36 control subjects were left for final analyses. Demographic information is presented in Table 1.

Neuropsychologic Testing

All participants underwent a battery of eight neuropsychologic tests to assess general mental status and other cognitive domains, including processing speed, verbal and nonverbal episodic memory, working memory, executive

function, reasoning, and language ability, as detailed in Appendix E1 (online). Neuropsychologic characterizations for each group are shown in Table 1.

MR Imaging Data Acquisition and Preprocessing

MR imaging data were acquired with a 3-T imager (Trio; Siemens, Erlangen, Germany) at the Imaging Center for Brain Research, Beijing Normal University. In all subjects, we obtained T1-weighted MR images (176 sagittal sections; section thickness, 1 mm; field of view, 256 × 256 mm; acquisition matrix, 256 × 256) and diffusion-weighted MR images (70 axial sections; section thickness, 2 mm; no section gap; 30 diffusion directions with a *b* value of 1000 sec/mm² and an additional image with a *b* value of 0 sec/mm²; field of view, 256 × 256 mm; acquisition matrix, 128 × 128; number of signals acquired, three). Imaging was performed by a physician with 12 years of experience in the acquisition of MR images. All images were reviewed,

Table 1

Characteristics of All Participants and Neuropsychologic Test Results

Characteristic	Control Subjects (n = 36)	Patients with SD aMCI (n = 18)	Patients with MD aMCI (n = 20)	F Value	P Value
Age (y)	63.1 ± 5.3	64.8 ± 7.2	65.4 ± 7.3	0.97	.38
Education (y)	11.2 ± 2.5	11.2 ± 3.0	11.6 ± 2.8	0.11	.90
Sex (M/F)	17/19	10/8	9/11	0.48	.79*
MMSE score	28.4 ± 1.7	26.8 ± 1.3	25.6 ± 1.7	18.71	<.001 ^{†‡§}
Auditory verbal learning test score	6.3 ± 2.1	1.8 ± 1.6	2.00 ± 1.3	52.88	<.001 ^{†‡}
Rey-Osterrieth complex figure test					
Copy	33.4 ± 4.4	33.9 ± 1.8	32.2 ± 3.3	1.22	.30
Recall	15.7 ± 7.3	10.7 ± 7.1	8.7 ± 5.9	7.53	.001 ^{†‡}
Digit span	12.8 ± 2.0	11.3 ± 1.9	11.1 ± 2.9	5.09	.009 ^{†‡}
Digit Symbol Coding	36.5 ± 9.7	33.8 ± 6.8	25.4 ± 9.8	9.68	<.001 ^{‡§}
Executive function					
Trail-making test A time (sec)	54.8 ± 19.6	53.9 ± 14.5	81.2 ± 35.5	9.02	<.001 ^{‡§}
Trail-making test B time (sec)	155.1 ± 54.9	160.3 ± 32.4	232.9 ± 73.6	13.28	<.001 ^{‡§}
Similarities	17.3 ± 3.7	15.7 ± 3.3	13.0 ± 4.6	7.65	.001 ^{‡§}
Boston naming test	25.1 ± 2.8	24.1 ± 3.1	21.7 ± 3.6	7.75	<.001 ^{‡§}

Note.—Unless otherwise indicated, data are mean ± standard deviation. All patients and control subjects were matched for age, sex, and education. The comparison of characteristics and neuropsychological scores among three groups (patients with SD aMCI, patients with MD aMCI, and control subjects) were performed with separate one-way analysis of variance (ANOVA). Post hoc pairwise comparisons were performed by using *t* tests. *P* < .05 with Bonferroni correction indicated a significant difference.

* The *P* value for sex distribution in the three groups was obtained by using a χ^2 test.

[†] Post hoc paired comparisons showed significant group differences between control subjects and patients with SD aMCI.

[‡] Post hoc paired comparisons showed significant group differences between control subjects and patients with MD aMCI.

[§] Post hoc paired comparisons showed significant group differences between patients with SD aMCI and patients with MD aMCI.

and the WM disease was evaluated by an experienced neuroradiologist (J.Z., 15 years of experience in clinical radiology). Image preprocessing comprised the following steps: eddy current and motion artifact correction of diffusion-tensor imaging data, estimation of diffusion tensor, fractional anisotropy calculation, and diffusion tensor tractography. Tractography was performed in each subject to generate three-dimensional curves (streamlines) characterizing fiber tract connectivity (26) (DTI Studio 3.0; H. Jiang, S. Mori, Johns Hopkins University, Baltimore, Md) (Appendix E1). MR image analysis was performed by an experienced observer (N.S., 7 years of experience in MR image analysis).

Network Model and Analysis

WM connectivity was modeled as an unweighted network comprising a total of 90 nodes, defined by automated anatomic labeling (27). Each node represented a distinct gray matter region (Table E1 [online]), and pairs of nodes were joined by a link if they were interconnected via a sufficient number of streamlines. To define the network edges, we selected a threshold value, T , for the streamline number. More specifically, the network edges were defined as 1 if the streamline number between the two regions was larger than the threshold ($T = 3$ in our study) and 0 in all other instances, as in several previous studies (13,28–30); this is detailed in Appendix E1 (online).

To characterize WM structural network, several key measures were used. They are degree, global efficiency, local efficiency, shortest path length (L_p), clustering coefficient (C_p), and small worldness (31). The degree of a node is the number of edges linking to it. The shortest path length between two nodes is the minimum number of edges along the path that must be traversed to establish a connection. Global efficiency is the inverse of path length and is associated with how well a network supports parallel information transfer. Local efficiency and clustering coefficient are measures of the efficiency of local information transfer between

neighboring nodes. A network is said to be small world if it has similar shortest path lengths but higher clustering coefficients than degree-matched random networks. In other words, a small-world network has a normalized path length ($\lambda = L_p^{\text{real}} / L_p^{\text{rand}} \approx 1$) and normalized clustering ($\gamma = C_p^{\text{real}} / C_p^{\text{rand}} > 1$), where L_p^{real} and C_p^{real} are shortest path length and clustering coefficient of the real network, respectively, and L_p^{rand} and C_p^{rand} are mean shortest path length and clustering coefficient, respectively, of 500 matched random networks that preserve the same number of nodes, edges, and degree distribution as the real network. For each node, we examined its nodal efficiency. For detailed definitions of these network measures, see Appendix E1 (online).

Statistical Analysis

Statistical analysis was performed by two authors (N.S., Y.L.) using software (SPSS, version 13.0; SPSS, Chicago, Ill). Group differences in age, years of education, and neuropsychological scores were examined with one-way ANOVA. Post hoc pairwise t tests with Bonferroni correction for multiple comparisons were performed if ANOVA yielded significant results ($P < .05$). Sex data were analyzed by using a χ^2 test. For group effects in global network measures and regional efficiencies, comparisons were performed among three groups by using one-way ANOVA with post hoc pairwise t tests with Bonferroni correction, when needed ($P < .05$). For 90 brain regions, the false discovery rate was calculated for multiple comparison correction. To test the linear trend of altered global and local network metrics among three groups (in the order of patients with MD aMCI, patients with SD aMCI, and control subjects), we performed the trend ANOVA. Finally, we investigated the relationship between network metrics and neuropsychological test scores. To identify the neuropsychological correlations with specific brain regions, we examined only the nodes with significant group differences. Of note, the correlation analyses were performed separately for aMCI and control groups.

Results

Demographics and Neuropsychologic Testing

There were no significant differences in age ratio, sex ratio, or years of education among the three groups ($P > .30$). The degree of WM hyperintensity in patients did not differ from that in control subjects (data not shown). The MMSE scores were significantly higher in control subjects than in patients with SD ($P = .002$) or MD ($P < .001$) aMCI; however, patients with SD aMCI scored better than did patients with MD aMCI ($P = .028$). For neuropsychological testing scores, the group effects were significant for all cognitive domains, with the best performance in control subjects, intermediate performance in patients with SD aMCI, and worst performance in patients with MD aMCI. Comparison of neuropsychological test scores between the SD and MD aMCI groups revealed significant differences in processing speed, executive function, and reasoning and language ability but no differences in episodic or working memory (Table 1; Appendix E1 [online]).

Global Topology of the WM Structural Networks

Both control subjects and patients with aMCI showed small-world organization of WM networks expressed as $\gamma > 1$ and $\lambda \approx 1$ (Fig 1; Table E2 [online]) consistent with previous findings (18–20). Significant group effects in the network degree ($P = .012$), global efficiency ($P = .003$), absolute ($P = .002$) and normalized ($P = .001$) path lengths, and normalized clustering ($P = .026$) were observed among the three groups, with significant differences between patients with MD aMCI and control subjects (all $P < .01$) but not between patients with SD aMCI and control subjects. Between patients with SD aMCI and those with MD aMCI, significant differences in global efficiency ($P = .016$) and characteristic path length ($P = .011$) of the WM networks were found (Fig 1; Table E2 [online]). Moreover, a linear trend of these altered network metrics was significant across three groups

Figure 1

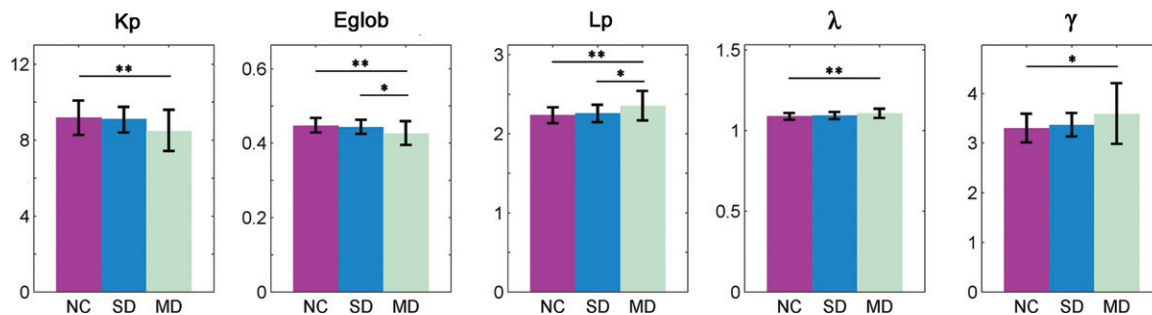


Figure 1: Group differences in global measures of WM structural networks were quantified among three groups. Bars and error bars represent mean values and standard deviations, respectively, of network properties in each group. MD = patients with MD aMCI, NC = control subjects, SD = patients with SD aMCI. Significant group effects in the network degree, global efficiency, absolute and normalized path lengths, and normalized clustering were observed among three groups (all $P < .05$). Post hoc comparisons showed decreased degree, decreased global efficiency, increased absolute and normalized path lengths, and increased normalized clustering in patients with MD aMCI relative to that in control subjects. There was no difference in healthy control subjects versus patients with SD aMCI in any of the global network measures. Moreover, patients with MD aMCI had significantly decreased global efficiency and increased absolute path length compared with patients with SD aMCI. * = Significant group difference at $P < .05$; ** = significant group difference at $P < .01$.

(all $P < .01$). At the threshold ($T = 3$), the sparsity of the WM network of each subject was around 10% (control subjects, $10.33\% \pm 0.93$; patients with SD aMCI, $10.25\% \pm 0.7$; patients with MD aMCI, $9.53\% \pm 1.18$).

Group Differences in Regional Efficiency

We further localized regions with reduced nodal efficiency in patients (Fig 2; Table 2). Regions with the most significant decreases were in the left ITG. Other disrupted regions were mainly distributed in the frontal and parietal cortices, including four frontal regions (right MFG, right SFG_{dor}, right SFG_{med}, and right supplementary motor area), five parietal regions (right supramarginal gyrus, right inferior parietal gyrus, right paracentral lobule, right postcentral gyrus, and left superior parietal gyrus), two paralimbic regions (bilateral ACG), and one subcortical region (left caudate nucleus). Post hoc tests revealed that all these regions had reduced efficiency in patients with MD aMCI versus control subjects. Between patients with SD aMCI and control subjects, only one region (right paracentral lobule) with reduced efficiency in patients was found. Moreover, four of these regions, including two frontal regions (right MFG and right SFG_{dor}),

Figure 2

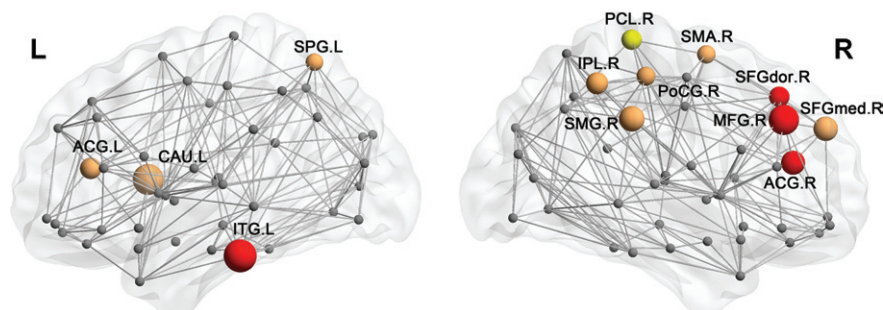


Figure 2: Schematic drawings show brain regions with significant group effects in nodal efficiency among three groups at $P < .05$ (false discovery rate corrected). Node sizes indicate the significance of between-group differences in regional efficiency. The network shown here was constructed by calculating the average of anatomic connection matrices of all healthy control subjects and the threshold with a sparsity of 10%. The nodal regions are located according to their centroid stereotaxic coordinates. Post hoc tests showed that all of these regions have reduced efficiency in patients with MD aMCI versus control subjects. Only one region (right paracentral lobule [PCL]) with reduced efficiency was found in patients with SD aMCI relative to control subjects (yellow). Moreover, four of these regions, including two frontal regions (right middle frontal gyrus [MFG], right dorsal superior frontal gyrus [SFG_{dor}]), one temporal region (left inferior temporal gyrus [ITG]), and one paralimbic region (right anterior cingulate gyrus [ACG]) showed reduced efficiency in patients with MD aMCI compared with that in patients with SD aMCI (red). CAU = caudate nucleus; IPL = inferior parietal, but supramarginal and angular gyri; PoCG = postcentral gyrus; SFG_{med} = medial superior frontal gyrus; SMA = supplementary motor area; SMG = supramarginal gyrus; SPG = superior parietal gyrus.

one temporal region (left ITG), and one paralimbic region (right ACG) showed reduced efficiencies in patients with MD aMCI as compared with those with SD aMCI. Note that ANOVA results were at the level of $P < .05$ after false discovery rate correction for 90 brain regions.

Correlations between Network Metrics and Neuropsychologic Tests

We examined the relationship between network metrics and neuropsychologic performance. For nodal characteristics, we examined only the nodes with significant group effects (ie, 13 regions

Table 2

Brain Regions with Significant Group Effects in Nodal Efficiency among Control Subjects, Patients with SD aMCI, and Patients with MD aMCI

Region	Category	F Value of ANOVA	T Value of Post Hoc Test		
			Control vs SD aMCI	Control vs MD aMCI	SD aMCI vs MD aMCI
Left ITG	Association	7.21 (.001)	NS	-3.74 (.0004)	-2.66 (.012)
Left CAU	Subcortical	6.98 (.002)	NS	-3.73 (.0005)	NS
Right MFG	Association	6.91 (.002)	NS	-3.25 (.002)	-3.07 (.004)
Right SMG	Association	6.36 (.003)	NS	-3.68 (.0005)	NS
Right SFG _{med}	Association	6.23 (.003)	NS	-3.34 (.002)	NS
Right ACG	Paralimbic	6.18 (.003)	NS	-2.84 (.006)	-3.15 (.003)
Right IPL	Association	5.95 (.004)	NS	-3.49 (.001)	NS
Left ACG	Paralimbic	5.88 (.004)	NS	-3.50 (.0009)	NS
Right SFG _{dor}	Association	5.77 (.005)	NS	-2.62 (.011)	-2.75 (.009)
Right PCL	Association	5.76 (.005)	-2.54 (.014)	-3.26 (.002)	NS
Right PoCG	Primary	5.60 (.006)	NS	-3.28 (.002)	NS
Right SMA	Association	5.53 (.006)	NS	-3.17 (.003)	NS
Left SPG	Association	5.43 (.006)	NS	-3.39 (.001)	NS

Note.—Data in parentheses are *P* values. The comparisons of nodal efficiency were performed among three groups (patients with SD aMCI, patients with MD aMCI, and control subjects) by using one-way ANOVA. Post hoc pairwise comparisons were then performed by using *t* tests. For ANOVA of 90 brain regions, $P < .05$ (false discovery rate corrected) was considered indicative of a significant difference. For post hoc tests, $P < .05$ with Bonferroni correction was considered indicative of a significant difference. CAU = caudate nucleus, IPL = inferior parietal, but supramarginal and angular gyri, NS = not significant, PCL = paracentral lobule, PoCG = postcentral gyrus, SMA = supplementary motor area, SMG = supramarginal gyrus.

in Table 2). In the control group, no correlation between neuropsychologic performances and network measures was found. In the aMCI group, the MMSE scores were negatively correlated with normalized clustering ($r = -0.37$, $P = .023$) and small worldness ($r = -0.37$, $P = .021$) (Fig 3a). The Digit Symbol Coding scores of the processing speed tests were correlated with degree ($r = 0.45$, $P = .004$), absolute path length ($r = -0.46$, $P = .004$), efficiency metrics (global efficiency: $r = 0.48$, $P = .002$; local efficiency: $r = 0.32$, $P = .047$) (Fig 3b), and nodal efficiency of the right SFG_{med} ($r = 0.52$, $P = .0008$) and right SFG_{dor} ($r = 0.51$, $P = .001$) (Fig 4a). Finally, the Trail Making Test B time of execution function tests was correlated with the degree ($r = -0.52$, $P = .0008$), absolute path length ($r = 0.42$, $P = .008$), efficiency metrics (global efficiency: $r = -0.44$, $P = .006$; local efficiency: $r = -0.41$, $P = .010$) (Fig 3c), nodal efficiency of the bilateral ACG (left: $r = -0.54$, $P = .0005$; right: $r = -0.51$, $P = .001$), right SFG_{med} ($r = -0.53$, $P < .0006$), and right SFG_{dor} ($r = -0.48$, $P = .002$) (Fig 4b). Note that for nodal correlations,

the Bonferroni correction was used for $P < .05$.

Discussion

The present study yielded evidence for disrupted topological organization of WM networks primarily in patients with MD aMCI, representing aberrant interconnections between pairs of gray matter regions. These impaired regions were distributed in the temporal, frontal, and parietal cortices. Importantly, the abnormalities were associated with the severity of aMCI as measured with MMSE and cognitive performances, implicitly suggesting the use of network properties as AD risk markers.

The spatial distribution of impaired brain regions in patients with MD aMCI was similar to the abnormalities in patients with early AD aMCI (6,32–35). The node with the greatest disruption was the left ITG, a region implicated in the pathophysiology of AD and MCI (34,36). Several structural MR imaging studies have consistently shown gray matter loss focused in the medial and inferior temporal lobes both in patients with SD aMCI and in patients with MD

aMCI (9,11). Our study provides evidence that the WM connections with ITG are altered in patients with aMCI. Although the concurrent abnormalities in gray matter (as reported in the literature) and the WM connections in the same brain region cannot be interpreted as the existence of possible causal relationships, we believe such strong association could generate new hypotheses to be examined further. More importantly, it raises the question of simultaneously considering both gray matter loss and disconnection of WM fibers to explore their relationship or integrate these two features to construct an MR imaging–based biomarker with higher sensitivity. While the ITG has been implicated in MCI and AD, we did not find a difference in the hippocampus or parahippocampal gyrus (a structure clearly involved in memory in AD and aMCI). A possible reason is that it is difficult to accurately reconstruct WM connections of the hippocampus and parahippocampus with deterministic tractography because of the limited image resolution. Another possible reason is that the patients with aMCI in this study had a milder stage

Figure 3

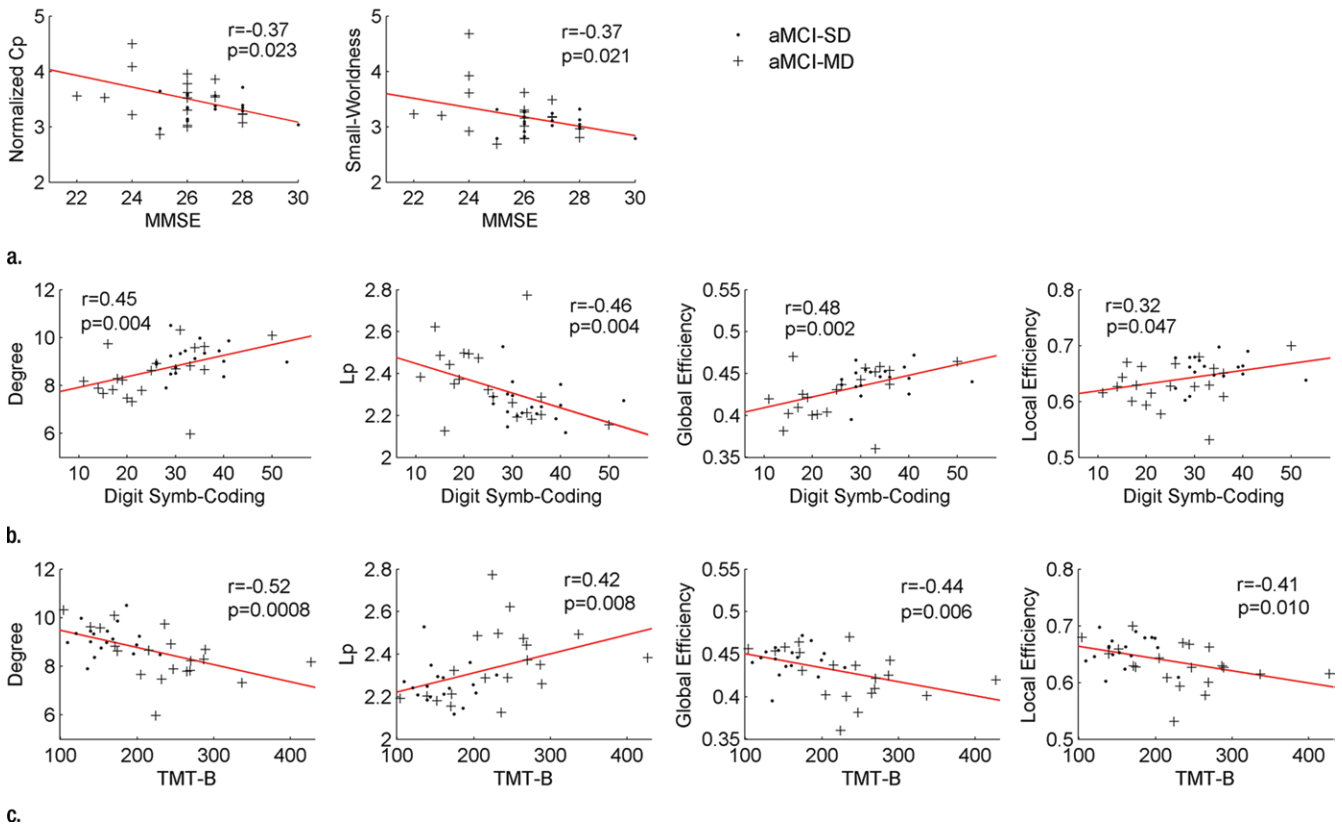


Figure 3: Plots show correlation between global network measures and neuropsychological scores in patients with aMCI. **(a)** Significant decreases of the normalized clustering and small worldness of the network with MMSE scores. **(b)** Significant increases of degree and global and local efficiencies and decreases of absolute path length of the network with Digit Symbol Coding scores of processing speed tests. **(c)** Significant decreases of degree and global and local efficiencies and increases of absolute path length of the network with the trail-making test B (*TMT-B*) time of execution function tests. *Cp* = clustering coefficient, *Lp* = shortest path length.

of cognitive impairment and were younger than patients with aMCI in previous studies (37,38). Thus, a future study with an adequate design needs to address this issue.

It is also interesting to note gray matter atrophy in the subcortical structure caudate nucleus reported for both MCI and AD (39–41). Discussions existed on the possible relationship between the impaired WM connections to this subcortical gray matter region with either vascular disease or cholinergic fiber degenerations (6). Another region with important findings is the anterior cingulate gyrus, which was shown to have a metabolic decrease in patients with MCI (42) and disruptions related to WM tract–cingulum bundles both in patients with AD and in patients

with MCI (43,44). In addition, the altered connectivity of frontal regions (ie, MFG, SFG_{dor}, and SFG_{med}) in patients with aMCI is also in agreement with the findings of a recent WM network study of AD (20). Moreover, the gray matter nodes with impaired connections in the lateral parietal cortex (paracentral lobule, supramarginal gyrus, and inferior parietal gyrus) and prefrontal cortex (SFG_{dor}, SFG_{med}, MFG, and ACG) are regions of the default mode network whose malfunction in patients with AD and MCI was discussed in previous reports (45,46). Thus, the current findings provided evidence to support the default mode network degeneration hypothesis (47) from the perspective of structural connectivity. Although the similarity of the alterations between

patients with MD aMCI and those with AD was not evaluated quantitatively or statistically, the diffused alterations in patients with MD aMCI most likely reflect the MD cognitive impairment and perhaps suggest that patients with MD aMCI are at higher risk for conversion to AD than are patients with SD aMCI (12). This possibility is supported by the lower neuropsychologic scores and by the increased mortality in patients with MD aMCI (48).

In patients with SD aMCI, we identified only one region (the right paracentral lobule) with reduced efficiency as compared with healthy control subjects. Sakamoto et al (49) found that patients with AD had a significant decrease in regional cerebral blood flow in the right paracentral lobule. Moreover,

Figure 4

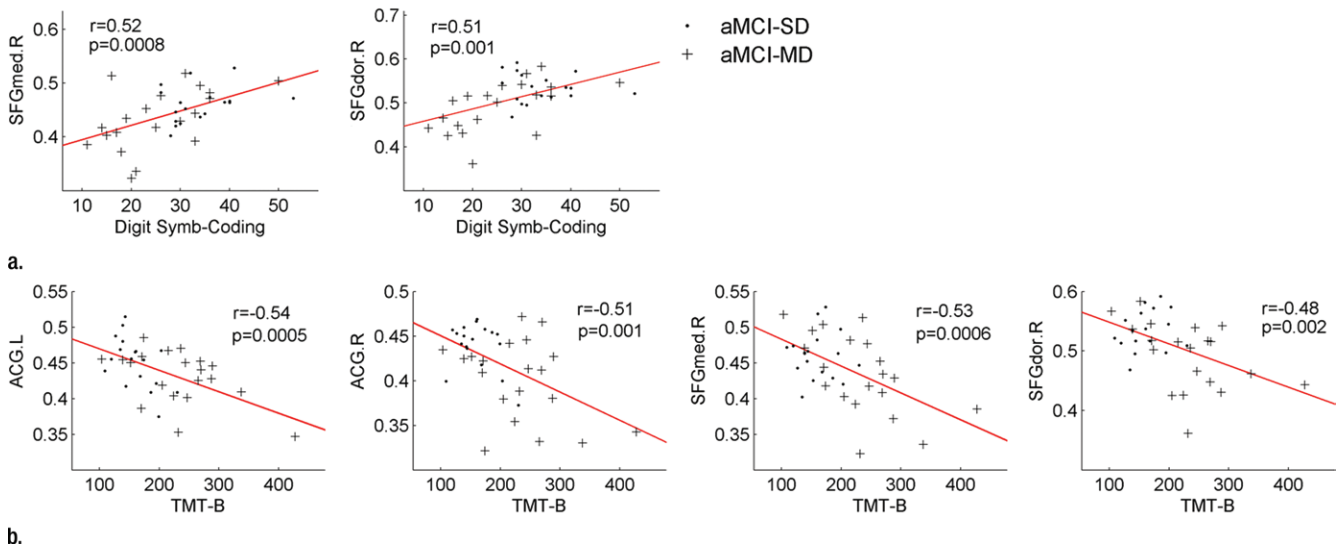


Figure 4: Plots show correlation between regional nodal efficiency and neuropsychological scores in patients with aMCI. **(a)** Significant increases of nodal efficiency in right SFG_{med} and right SFG_{dor} with Digit Symbol Coding scores of processing speed tests. **(b)** Significant decreases of nodal efficiency in the bilateral ACG, right SFG_{med} and right SFG_{dor} with the trail-making test B (*TMT-B*) time of execution function tests. For the abbreviations of nodes, see Table E1 (online).

the resting glucose metabolism in the right paracentral lobule was positively correlated with MMSE scores in patients with AD (50). However, morphologic studies showed gray matter loss focused in the medial temporal areas in patients with SD aMCI (9,11). Findings reported in the literature for fluorodeoxyglucose positron emission tomography (PET), amyloid PET (Pittsburgh compound B or florbetapir), and volumetric MR imaging pointed to brain regions differently dependent on whether it is functional, pathologic, or structural. There have been discussions about the relationships between different findings (32,51). The discrepancy might reflect the fact that our analysis indexed a distinct aspect of neuropathology—WM connectivity as opposed to gray matter volume.

The differences between patients with SD aMCI and those with MD aMCI were mainly located in the frontal cortex, with the most pronounced changes in the right ACG, MFG, and SFG_{dor}. These frontal regions are reportedly involved in emotional, memory, and executive functions (52,53). The more severe disruption of the frontal regions in patients with MD aMCI may be related to

the diffused cognitive dysfunction. In addition to the disrupted frontal region connections, the nodal efficiency of the disrupted parietal region was found to be monotonically associated with the disease severity (nodal efficiency in patients with MD aMCI was less than that in patients with SD aMCI, which in turn was less than that in control subjects) with trend ANOVA.

We first note that the MMSE score negatively correlated with small-worldness and network clustering in patients with aMCI. The small-world model reflects an optimal balance between local specialization and global integration. The clustering and small-worldness changes indicate a possible disruption of WM connections in patients with increased disease severity. We also found significant correlations of processing speed and executive function with decreased network efficiencies. Specifically, several frontal cortical areas (SFG_{med} and SFG_{dor}) with reduced efficiency showed strong correlations with the deficits in processing speed; several disrupted frontal and paralimbic regions (SFG_{med}, SFG_{dor}, and ACG) were significantly correlated with the impaired executive function. Correlation between executive function

and diffusion abnormalities in the anterior cingulum in older adults without dementia has been reported recently (54). Our findings show that the aberrant structural connectivity of these regions is related to the cognitive impairments of patients with aMCI from the brain connectome perspective. It is worth noting that our correlation results are also in line with the findings of a recent WM network study on aging, reporting association of the processing speed and executive functions with the efficiency of the WM network in elderly subjects (55). However, we did not find a neuropsychological correlation with global network measures for each aMCI subtype group, which may be due to a small sample size of the subgroups.

We are aware of several methodologic limitations of our study. First, we used deterministic tractography to define the WM network edges. This method has been used in several diffusion-tensor imaging studies (13,28–30). However, because of the fiber crossing problem and limitations of adequately tracking long-distance fibers (56), it might result in the loss of tracing existing fibers. There are different tractography methods (14) and advanced diffusion

imaging techniques (57,58) that could make the fiber pathway identifications more precise. Additional studies are needed with these alternatives to evaluate the reproducibility of our results. Second, we constructed an unweighted network. For a weighted network, several candidate measures—such as fiber numbers, mean fiber length, fiber density, and mean FA—have been proposed (15,20,30). In the present study, we also constructed fiber number-weighted and FA-weighted networks for each subject and obtained similar results (Appendix E1; Figs E4, E5 [online]). Third, it has been previously shown that brain graph metrics are dependent on the resolution of the network (network size) (59,60). Recent studies have suggested the use of higher-spatial-resolution networks of up to 1000 smaller parcels or of voxelwise level instead of the use of a coarse parcellation scheme of 90 brain regions (15,60). Thus, future studies with high-spatial-resolution network analysis should be performed to validate our findings. Fourth, we examined the network property differences cross sectionally and with unknown rates of conversion to AD. Thus, the assertion that MD aMCI has a higher risk for conversion to AD primarily is based on reported findings in the literature (12) and the correlation with neuropsychological and clinical tests. Longitudinal studies are needed to investigate the conversion of aMCI subtypes to AD and to evaluate clinical values of network metrics to predict AD or longitudinal changes. Finally, we found disrupted WM connectivity only in patients with aMCI; however, the relationship between alterations of gray matter and WM are still unclear. The effects in the connectivity will probably be due to cell loss of gray matter, in which the WM is involved only secondarily. Thus, in future studies, it will be necessary to establish WM connectivity as an independent factor, or multivariable analysis will be performed to explore the relationship between WM and gray matter changes in patients with these disorders.

Acknowledgments: We thank the participating sites in the Clinic at Neurology Department of Beijing Hospital and the Clinic at China Acad-

emy of Chinese Medicine. We thank all the volunteers and patients for their participation in the study. We also thank Mingrui Xia, MS, for network visualization.

Disclosures of Conflicts of Interest: N.S. No relevant conflicts of interest to disclose. Y.L. No relevant conflicts of interest to disclose. H.L. No relevant conflicts of interest to disclose. J.Z. No relevant conflicts of interest to disclose. X.L. No relevant conflicts of interest to disclose. L.W. No relevant conflicts of interest to disclose. Y.H. No relevant conflicts of interest to disclose. Y.W. No relevant conflicts of interest to disclose. Z.Z. No relevant conflicts of interest to disclose.

References

- Petersen RC, Smith GE, Waring SC, Ivnik RJ, Tangalos EG, Kokmen E. Mild cognitive impairment: clinical characterization and outcome. *Arch Neurol* 1999;56(3):303–308.
- Petersen RC, Stevens JC, Ganguli M, Tangalos EG, Cummings JL, DeKosky ST. Practice parameter: early detection of dementia—mild cognitive impairment (an evidence-based review). Report of the Quality Standards Subcommittee of the American Academy of Neurology. *Neurology* 2001;56(9):1133–1142.
- Winblad B, Palmer K, Kivipelto M, et al. Mild cognitive impairment: beyond controversies, towards a consensus—report of the International Working Group on Mild Cognitive Impairment. *J Intern Med* 2004;256(3):240–246.
- Bai F, Zhang Z, Watson DR, et al. Abnormal functional connectivity of hippocampus during episodic memory retrieval processing network in amnesic mild cognitive impairment. *Biol Psychiatry* 2009;65(11):951–958.
- Apostolova LG, Dinov ID, Dutton RA, et al. 3D comparison of hippocampal atrophy in amnesic mild cognitive impairment and Alzheimer's disease. *Brain* 2006;129(Pt 11):2867–2873.
- Chua TC, Wen W, Slavin MJ, Sachdev PS. Diffusion tensor imaging in mild cognitive impairment and Alzheimer's disease: a review. *Curr Opin Neurol* 2008;21(1):83–92.
- Becker JT, Davis SW, Hayashi KM, et al. Three-dimensional patterns of hippocampal atrophy in mild cognitive impairment. *Arch Neurol* 2006;63(1):97–101.
- Bell-McGinty S, Lopez OL, Meltzer CC, et al. Differential cortical atrophy in subgroups of mild cognitive impairment. *Arch Neurol* 2005;62(9):1393–1397.
- Seo SW, Im K, Lee JM, et al. Cortical thickness in single- versus multiple-domain amnesic mild cognitive impairment. *Neuroimage* 2007;36(2):289–297.
- He J, Farias S, Martinez O, Reed B, Mungas D, Decarli C. Differences in brain volume, hippocampal volume, cerebrovascular risk factors, and apolipoprotein E4 among mild cognitive impairment subtypes. *Arch Neurol* 2009;66(11):1393–1399.
- Whitwell JL, Petersen RC, Negash S, et al. Patterns of atrophy differ among specific subtypes of mild cognitive impairment. *Arch Neurol* 2007;64(8):1130–1138.
- Busse A, Hensel A, Gühne U, Angermeyer MC, Riedel-Heller SG. Mild cognitive impairment: long-term course of four clinical subtypes. *Neurology* 2006;67(12):2176–2185.
- Gong G, He Y, Concha L, et al. Mapping anatomical connectivity patterns of human cerebral cortex using in vivo diffusion tensor imaging tractography. *Cereb Cortex* 2009;19(3):524–536.
- Zalesky A, Fornito A. A DTI-derived measure of cortico-cortical connectivity. *IEEE Trans Med Imaging* 2009;28(7):1023–1036.
- Hagmann P, Cammoun L, Gigandet X, et al. Mapping the structural core of human cerebral cortex. *PLoS Biol* 2008;6(7):e159.
- Bullmore E, Sporns O. Complex brain networks: graph theoretical analysis of structural and functional systems. *Nat Rev Neurosci* 2009;10(3):186–198.
- He Y, Evans A. Graph theoretical modeling of brain connectivity. *Curr Opin Neurol* 2010;23(4):341–350.
- He Y, Chen Z, Evans A. Structural insights into aberrant topological patterns of large-scale cortical networks in Alzheimer's disease. *J Neurosci* 2008;28(18):4756–4766.
- Yao Z, Zhang Y, Lin L, et al. Abnormal cortical networks in mild cognitive impairment and Alzheimer's disease. *PLOS Comput Biol* 2010;6(11):e1001006.
- Lo CY, Wang PN, Chou KH, Wang J, He Y, Lin CP. Diffusion tensor tractography reveals abnormal topological organization in structural cortical networks in Alzheimer's disease. *J Neurosci* 2010;30(50):16876–16885.
- Supekar K, Menon V, Rubin D, Musen M, Greicius MD. Network analysis of intrinsic functional brain connectivity in Alzheimer's disease. *PLOS Comput Biol* 2008;4(6):e1000100.
- Zhang MY, Katzman R, Salmon D, et al. The prevalence of dementia and Alzheimer's disease in Shanghai, China: impact of age, gender, and education. *Ann Neurol* 1990;27(4):428–437.
- Petersen RC. Mild cognitive impairment as a diagnostic entity. *J Intern Med* 2004;256(3):183–194.

24. Guo Q, Zhao Q, Chen M, Ding D, Hong Z. A comparison study of mild cognitive impairment with 3 memory tests among Chinese individuals. *Alzheimer Dis Assoc Disord* 2009;23(3):253–259.
25. Zhang MY, Elena Y, He YL. Activities of daily living scale. *Shanghai Arch Psychiatry* 1995;7:3.
26. Mori S, Crain BJ, Chacko VP, van Zijl PC. Three-dimensional tracking of axonal projections in the brain by magnetic resonance imaging. *Ann Neurol* 1999;45(2):265–269.
27. Tzourio-Mazoyer N, Landeau B, Papathanassiou D, et al. Automated anatomical labeling of activations in SPM using a macroscopic anatomical parcellation of the MNI MRI single-subject brain. *Neuroimage* 2002;15(1):273–289.
28. Zalesky A, Fornito A, Seal ML, et al. Disrupted axonal fiber connectivity in schizophrenia. *Biol Psychiatry* 2011;69(1):80–89.
29. Shu N, Liu Y, Li J, Li Y, Yu C, Jiang T. Altered anatomical network in early blindness revealed by diffusion tensor tractography. *PLoS ONE* 2009;4(9):e7228.
30. Shu N, Liu Y, Li K, et al. Diffusion tensor tractography reveals disrupted topological efficiency in white matter structural networks in multiple sclerosis. *Cereb Cortex* 2011;21(11):2565–2577.
31. Rubinov M, Sporns O. Complex network measures of brain connectivity: uses and interpretations. *Neuroimage* 2010;52(3):1059–1069.
32. Buckner RL, Snyder AZ, Shannon BJ, et al. Molecular, structural, and functional characterization of Alzheimer's disease: evidence for a relationship between default activity, amyloid, and memory. *J Neurosci* 2005;25(34):7709–7717.
33. Delbeuck X, Van der Linden M, Collette F. Alzheimer's disease as a disconnection syndrome? *Neuropsychol Rev* 2003;13(2):79–92.
34. Singh V, Chertkow H, Lerch JP, Evans AC, Dorr AE, Kabani NJ. Spatial patterns of cortical thinning in mild cognitive impairment and Alzheimer's disease. *Brain* 2006;129(Pt 11):2885–2893.
35. Agosta F, Pievani M, Sala S, et al. White matter damage in Alzheimer disease and its relationship to gray matter atrophy. *Radiology* 2011;258(3):853–863.
36. Pihlajamäki M, Jauhiainen AM, Soininen H. Structural and functional MRI in mild cognitive impairment. *Curr Alzheimer Res* 2009;6(2):179–185.
37. Wang Y, West JD, Flashman LA, et al. Selective changes in white matter integrity in MCI and older adults with cognitive complaints. *Biochim Biophys Acta* 2012;1822(3):423–430.
38. Liu Y, Spulber G, Lehtimäki KK, et al. Diffusion tensor imaging and tract-based spatial statistics in Alzheimer's disease and mild cognitive impairment. *Neurobiol Aging* 2011;32(9):1558–1571.
39. Madsen SK, Ho AJ, Hua X, et al. 3D maps localize caudate nucleus atrophy in 400 Alzheimer's disease, mild cognitive impairment, and healthy elderly subjects. *Neurobiol Aging* 2010;31(8):1312–1325.
40. Spampinato MV, Rumboldt Z, Hosker RJ, Mintzer JE; Alzheimer's Disease Neuroimaging Initiative. Apolipoprotein E and gray matter volume loss in patients with mild cognitive impairment and Alzheimer disease. *Radiology* 2011;258(3):843–852.
41. Skup M, Zhu H, Wang Y, et al. Sex differences in grey matter atrophy patterns among AD and aMCI patients: results from ADNI. *Neuroimage* 2011;56(3):890–906.
42. Fouquet M, Desgranges B, Landeau B, et al. Longitudinal brain metabolic changes from amnesic mild cognitive impairment to Alzheimer's disease. *Brain* 2009;132(Pt 8):2058–2067.
43. Zhang Y, Schuff N, Jahng GH, et al. Diffusion tensor imaging of cingulum fibers in mild cognitive impairment and Alzheimer disease. *Neurology* 2007;68(1):13–19.
44. Mielke MM, Kozauer NA, Chan KC, et al. Regionally-specific diffusion tensor imaging in mild cognitive impairment and Alzheimer's disease. *Neuroimage* 2009;46(1):47–55.
45. Sorg C, Riedel V, Mühlau M, et al. Selective changes of resting-state networks in individuals at risk for Alzheimer's disease. *Proc Natl Acad Sci U S A* 2007;104(47):18760–18765.
46. Qi Z, Wu X, Wang Z, et al. Impairment and compensation coexist in amnesic MCI default mode network. *Neuroimage* 2010;50(1):48–55.
47. Seeley WW, Crawford RK, Zhou J, Miller BL, Greicius MD. Neurodegenerative diseases target large-scale human brain networks. *Neuron* 2009;62(1):42–52.
48. Hunderfund AL, Roberts RO, Slusser TC, et al. Mortality in amnesic mild cognitive impairment: a prospective community study. *Neurology* 2006;67(10):1764–1768.
49. Sakamoto S, Matsuda H, Asada T, et al. Apolipoprotein E genotype and early Alzheimer's disease: a longitudinal SPECT study. *J Neuroimaging* 2003;13(2):113–123.
50. Bokde ALW, Teipel SJ, Drzezga A, et al. Association between cognitive performance and cortical glucose metabolism in patients with mild Alzheimer's disease. *Dement Geriatr Cogn Disord* 2005;20(6):352–357.
51. Klunk WE, Engler H, Nordberg A, et al. Imaging brain amyloid in Alzheimer's disease with Pittsburgh Compound-B. *Ann Neurol* 2004;55(3):306–319.
52. Baddeley A. Working memory: looking back and looking forward. *Nat Rev Neurosci* 2003;4(10):829–839.
53. Stuss DT, Alexander MP. Executive functions and the frontal lobes: a conceptual view. *Psychol Res* 2000;63(3-4):289–298.
54. Kantarci K, Senjem ML, Avula R, et al. Diffusion tensor imaging and cognitive function in older adults with no dementia. *Neurology* 2011;77(1):26–34.
55. Wen W, Zhu W, He Y, et al. Discrete neuroanatomical networks are associated with specific cognitive abilities in old age. *J Neurosci* 2011;31(4):1204–1212.
56. Mori S, van Zijl PC. Fiber tracking: principles and strategies—a technical review. *NMR Biomed* 2002;15(7-8):468–480.
57. Tuch DS. Q-ball imaging. *Magn Reson Med* 2004;52(6):1358–1372.
58. Wedeen VJ, Hagmann P, Tseng WY, Reese TG, Weisskoff RM. Mapping complex tissue architecture with diffusion spectrum magnetic resonance imaging. *Magn Reson Med* 2005;54(6):1377–1386.
59. Zalesky A, Fornito A, Harding IH, et al. Whole-brain anatomical networks: does the choice of nodes matter? *Neuroimage* 2010;50(3):970–983.
60. van den Heuvel MP, Stam CJ, Boersma M, Hulshoff Pol HE. Small-world and scale-free organization of voxel-based resting-state functional connectivity in the human brain. *Neuroimage* 2008;43(3):528–539.